NANOMATERIALS BASED ON POLY (3-HYDROXYBUTYRATE) – PHYSICOCHEMICAL, MECHANICAL AND BIOLOGICAL STUDIES

[1]ANNA CZERNIECKA-KUBICKA, [2]ANGELIKA KAMIZELA, [3]AGNIESZKA SZYSZKOWSKA1, [4]KAROLINA MATERNIA-DUDZIK1, [5]WERONIKA GONCIARZ, [6]KAMIL GANCARCZYK, [7]IWONA ZARZYKA

[1,2,3,4] Medical College of Rzeszow University, University of Rzeszow, Poland
[5]Department of Immunology and Infectious Biology, Institute of Microbiology, Biotechnology and Immunology, Faculty of Biology and Environmental Protection, University of Łódź, 90-237 Łódź, Poland
[6]Department of Material Science, Faculty of Mechanical Engineering and Aeronautics, Rzeszow University of Technology, 35-959 Rzeszow, Poland
[7]Department of Chemistry, Rzeszow University of Technology, 35-959, Rzeszow, Poland
E-mail: [1]aczerniecka@ur.edu.pl, [2]angelikakamizela@gmail.com, [3]szyszkowska.agnieszka@gmail.com, [4]kmaternia@ur.edu.pl, [5]weronika.gonciarz@biol.uni.lodz.pl, [6]kamilgancarzyk@prz.edu.pl, [7]izarzyka@prz.edu.pl

Abstract - The poly (3-hydroxybutyrate), P3HB, was used to prepare biocompatible composites modified by the nanocrystalline cellulose. The aim of the study was to assess selected thermal, mechanical, and biological properties of the obtained nanocomposites. The crystallinity of nanocomposites and polymeric matrix were investigated using X-ray spectra. The immunosafety of the tested nanocomposites and the absence of, or very low, endotoxin contamination was confirmed by the the Food and Drug Agency Guidance as well as the European Medicines Agency. Some mechanical properties of the investigated materials were also measured and presented. It was estimated that the addition of 1% by mass of nanocrystalline cellulose to P3HB causes the greatest progress in the plasticization of the material, which is characterized by the best processing and utility properties. The processing window of P3HB-1 was extended by approx. 25°C in reference to the unfilled P3HB.

Keywords - Nanocomposites, Poly(3-Hydroxybutyrate), Nanocrystalline Cellulose, Biocompatibility

I. INTRODUCTION

Poly-3-hydroxybutyrate (P3HB) belonging to poly hydroxyalkanoates (PHA) is an isotactic polyester of 3-(R)-hydroxybutyric acid displaying the shape memory effect and thus included in the group of smart materials. Shape memory materials have the ability to regain their original form under the influence of a stimulus such as energy in the form of heat, light, magnetic and electric fields, ultrasounds or chemical agents [1].

Most often, however, chemical compounds are used, for which temperature is the triggering factor for returning to the original shape. The mechanism of thermal shape memory SMP (Shape Memory Polymers) results from thermal transformations of polymers. It can be a glass transition characterized by the glass transition temperature, T_g, or the melting process of the crystalline phase at a temperature defined by the melting temperature, T_m. For homopolymers, such transitions determine the temperature range of polymer applicability: amorphous polymers above T_g, crystalline polymers above T_m, lose their utility properties. Moreover, for crystalline polymers, the glass transition occurs over a wide temperature range and depends on the thermal history of the polymer. Compared to the commonly used metal alloys SMA (Shape Memory Alloys), polymers with this property are less expensive to produce, and the adjustment of the return temperature of the shape change is simpler than for SMA. For this reason, SMPs are slowly displacing SMAs not only in industry, but also in medicine [2].

They are used, among others things, for the production of controlled drug release systems [3], the production of implants, surgical threads, lenses, cardiovascular and urological stents [4, 5] and the repair of bone defects [6] and cartilage [7].

The intensity of research currently conducted in this direction allows us to assume that in the near future there will be many more of these applications.

An ideal polymer for biomedical applications should be characterized by appropriate biocompatibility, bioresorption and biodegradation. Taking these assumptions into account, thermoplastic polymers [8], whose representative is poly-3-hydroxybutyrate, work best in the production of biomaterials.

The natural method of obtaining this polymer is the fermentation of glucose carried out by many groups of microorganisms for which P3HB is a reserve material [9, 10]. Poly-3-hydroxybutyrate was first isolated from Bacillus megaterium in 1926. On an industrial scale, the fermentation reaction carried out by Alcaligenes Eutrophus is used [11]. In the biotransformation process, only one enantiomer of this compound is formed, so the product is characterized by a degree of crystallinity >95%. In addition to biocatalytic methods, there are also known methods of obtaining polyester by chemical synthesis [12, 13].

Due to its properties, P3HB is an attractive substrate for the production of biomedical materials. It is not toxic, and it is broken down in the body through hydrolysis reaction to the normally occurring metabolite - hydroxybutyric acid. It can also be

degraded in soil to carbon dioxide and water, in processes catalyzed by microorganisms [14].
The degree of crystallinity of the polymer depends on the cooling rate and is usually in the range of 50-80%. The glass transition temperature of semi-crystalline P3HB is 273-300 K, and the melting process is observed in the range of 453-463K [15].The aim of this paper is to obtain new nanocomposites based on P3HB and nanocrystalline cellulose and to study their properties in order to determine their utility applications.

II. EXPERIMENTAL SECTION

2.1. Materials

Poly (3-hydroxybutyrate), P3HB, was supplied by Biomer (Krailling, Germany). Weight average molecular mass of P3HB is M_w = 443,900 g/mol and its dispersity $M_w \cdot M_n^{-1}$ = 5.72 measured by the size exclusion chromatography in chloroform.
P3HB melt flow index is 0.11 g· (10 min)$^{-1}$ (180°C at 2.16 kg). The molar mass of the repeating unit equals 86.09 g/mol. Nanocrystalline cellulose, CNC, was supplied by Nanografi Nanotechnology (Ankara,Turkey), CAS number: 9004-34-6, average particle size of nanocrystalline cellulose is 10-20 nm wide, 300-900 nm length. The average density is 1.49 g/cm^3. Decomposition temperature of nanocrystalline cellulose (TGA in N_2) is 349 °C. Crystallinity of cellulose (XRD) is 92%.

III. METHODS AND INSTRUMENTATION

3.1. Nanobiocomposites preparation

The nanocomposites were prepared by melt mixing of P3HB with different amounts of nanocrystalline cellulose i.e. 0.5, 1, 2, and 3 mass % in co-rotating twin-screw micro-extruder. Before extrusion, the nanofiller was homogenized with the polymeric matrix using an electric grinder.
The conditions of the melt mixing and full characterization of nanocomposite samples based on P3HB and nanofiller (nanocrystalline cellulose) were given in Table 1. Unfilled P3HB was also meltmixed to prepare a reference material. Sample abbreviations and content of hypromellose are given in Table 1.

Sample designation	Content of hypromellose	Temperature of extrusion	Speed of rotation
P3HB	0	Zone 1: 125°C Zone 2: 135°C Zone 3: 150°C Zone 4: 160°C Head: 166°C	350 rpm
P3HB-0.5	0.5		
P3HB-1	1		
P3HB-2	2		
P3HB-3	3		

Table 1. Sample abbreviations and preparation conditions of obtained nanocomposites

3.2. Thermo gravimetry

Thermo gravimetric analysis (TGA) was performed using a Metler Toledo TGA/DSC 3+ thermogravimetric analyzer. The samples were heated at a heating rate of 5°C/min in the temperature range of 25-600°C in an inert gas (nitrogen) atmosphere

3.3. Differential scanning calorimetry

All experiments by calorimetry in the temperature range from -90°C to 195°C were performed using a differential scanning calorimeter (DSC), Q1000™, from TA Instruments, Inc. (New Castle, DE, USA). This calorimeter is the heat-flux type and is equipped with a mechanical refrigerator to control heating and cooling of samples. Measurements were carried out in a nitrogen atmosphere with a constant flow rate of around 50 ml/min. The mass of the samples used for measurements by DSC was about 10 mg. The experimental heat flow rates were measured at a heating rate of 10°C /min after the previous cooling at a rate of 10°C/min by standard DSC. The temperature and heat flow rate calibration in the DSC apparatus was performed using parameters of melting indium, onset melting temperature, T_m(onset) = 156.6°C, and heat of fusion, ΔH_f = 28.45 J/g (3.281 kJ/mol). In order to obtain accurate results, the heat capacity was calibrated by sapphire. The heat flow data were collected from the second heating run after the controlled cooling.

3.4. X-rays

Phase composition of the samples were identified using an X-ray diffractometer Miniflex II from Rigaku company. Filtered copper lamp (CuKα,λ = 0,1542 nm), with a voltage of 40 kV, range 2θ = 3-30° and step size 0,02°/3s was used.

IV. BIOLOGICAL STUDY

4.1. Cell culture and in vitro biocompatibility assessment

Reference L929 mouse fibroblasts (LGC Standards, Middlesex, UK), human Hs68 skin fibroblasts (CRL-1635™) were used to evaluate the biocompatibility of tested materials in vitro. Mouse L929 fibroblasts were cultured at 37°C in a 5% CO2 in Roswell Park Memorial Institute (RPMI)-1640 medium (Biowest, Nuaillé, France), supplemented with 10% heat-inactivated fetal bovine serum (FBS) (Biowest, Nuaillé, France), and standard antibiotics: penicillin (100 U/mL) and streptomycin (100 µg/mL) (Biowest, Nuaillé, France), while the human fetal osteoblastic cell line hFOB 1.19 (CRL-11372™) obtained from the American Type Culture Collection (ATCC, Manassas, VA, USA), were cultured in a 1:1 mixture of phenol-free Dulbecco's modified Eagle's medium and Ham's 12-F medium (Gibco, Thermo Fisher Scientific, Waltham, MA, USA) supplemented with 2.5 mL of l-glutamine (Biowest, Nuaillé, France), 10% heat inactivated FBS (Biowest, Nuaillé, France) and 0.3 mg/mL of geneticin (G418) (Sigma-Aldrich, Saint Louis, MO, USA), whereas human bone osteosarcoma Saos-2 (HTB-85™, ATTC) were cultured in McCoy's 5A Medium (Biowest, Nuaillé,

France) supplemented with 15% heat-inactivated FBS (Biowest, Nuaillé, France), and standard antibiotics: penicillin (100 U/mL) and streptomycin (100 µg/mL) (Biowest, Nuaillé, France),was used in this study. Cell cultures were supplemented with fresh medium two or three times per week to keep them in log phase. The confluent monolayer was treated with 0.25% trypsin-EDTA solution (Biowest, Nuaillé, France) to passage. Cytotoxicity of the P3HB, P3HB-0.5, P3HB-1.0, P3HB-2.0, P3HB-3.0 was tested using L929, hFOB 1.19 and Saos-2 cell line (density of 2×105 cells/mL) according to the ISO norm 10993–5 (International Organization for Standardization, 2009; Biological evaluation of medical devices—Part 5: Tests for in vitro cytotoxicity), based on the 3-(4,5-dimethylthiazol-2-yl)-2,5-diphenyltetrazolium bromide (MTT) reduction test, as previously described [16]. For cytotoxicity testing P3HB, P3HB-0.5, P3HB-1, P3HB-2, P3HB-3, corresponding to one-tenth of the well surface area, were prepared. The cell cultures in medium alone, without the P3HB, P3HB-0.5, P3HB-1, P3HB-2, P3HB-3, were used as a positive control (PC) for cell viability, whereas cells treated with 0.03% H_2O_2 were used as a negative control (NC), i.e. 100% dead cells due to lysis. The absorbance was measured spectrophotometrically using a Multiskan EX plate reader (Thermo Scientific, Waltham, MA, USA) at 570 nm. MTT reduction relative to untreated cells (%) = (absorbance of treated cells/absorbance of untreated cells × 100%)×100%. The above-mentioned tests were performed in three independent experiments.

4.2. Monocyte Activation Assay

ThP1-Blue™ cells (Invitrogen, San Diego, CA, USA), derived from the human THP-1 monocyte cell line, were used to assess whether the P3HB, P3HB-0.5, P3HB-1, P3HB-2, P3HB-3, could stimulate monocytes through induction of nuclear factor kappa B (NF-κB). THP1-Blue™ cells were derived from the human THP-1 monocyte cell line by stable integration of anNF-κB-inducible embryonic alkaline phosphatase (SEAP) reporter construct. Activation of NF-κB resulted in the secretion of SEAP, which could be detected spectrophotometrically using Quanti-Blue reagent (Invitrogen, San Diego, CA, USA).THP1-Blue™ cells were cultured at 37 °C in a 5% CO2 in RPMI-1640 medium supplemented with 10% FBS, 25 mM 4-(2-hydroxyethyl)-1-piperazine-ethanesulfonic acid (HEPES), penicillin/streptomycin (100 U/mL), and 2 mM glutamine (all from Biowest,Nuaillé, France), as well as blastidin (10 µg/mL) (Invitrogen, San Diego, CA, USA), as previously described [17]. For monocyte activation assay THP-1 Blue™ cells (density of 5×105 cells/mL) stimulated with P3HB, P3HB-0.5, P3HB-1, P3HB-2, P3HB-3 prepared as described above. Untreated cells in culture medium alone served as a negative control, whereas cells treated with Escherichia coli lipopolysaccharide (LPS) (1 µg/mL) (Sigma-Aldrich, St. Louis, MO, USA) were taken as a positive control. The SEAP activity was measured spectrophotometrically using a Multiskan EX plate reader (Thermo Scientific, Waltham, MA, USA) at 650 nm. The above-mentioned tests were performed in three independent experiments.

4.3. Statistical analysis

Statistical significance was accepted at a p-value < 0.05 nonparametric U Mann-Whitney. Data are presented as mean values ± SD. For statistical analysis the STATISTICA 123PL software was used (Stat Soft, Poland).

4.4. Mechanical tests

The mechanical properties of the obtained nanobiocomposites and the unfilled P3HB were tested, i.e. tensile strength, elongation at break, impact strength by Charpy method and Shore hardness. The tensile strength and strain at break were determined in accordance with the standard [PN-EN ISO 527-1: 2020-01]. The test was carried out at a jaw feed rate of 50 mm / min. Charpy impact tests on notched samples were carried out with the IMPats-15/50, ATSFAAR S. p. A. hammer in accordance with the standard [PN-EN ISO 179-1: 2010]. Shore hardness tests were made in accordance with the [PN-ISO 868:1998] standard with the use of Zwick Roell equipment. The scale D has been applied.

V. RESULTS AND DISCUSSION

Figure 1 shows X-ray diffractograms of the unfilled P3HB and its nanocomposites with nanocrystalline cellulose. The diffractograms indicate a gradient of increased resolution and peak sharpness with an increased amount of nanocrystalline cellulose in composites. It is observed that the peak resolution increased in the range 2Θ from 19 to 24°. It indicates the growth of the crystallinity of the resulted nanocomposites due to the increase in crystal number as the nanocrystalline cellulose percentage rises.

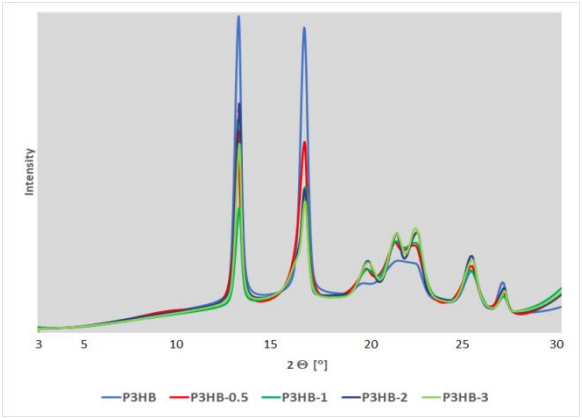


Fig.1. X-ray diffractograms recorded in transmission mode for unfilled P3HB, and composites containing 0.5 and 1, 2, and 3 wt.% nanocrystalline cellulose (designated P3HB-0.5, P3HB-1, P3HB-2, and P3HB-3, respectively).

The influence of the addition of nanocrystalline cellulose on the mechanical properties of the produced nanocomposites based on the P3HB matrix was also investigated. The tensile strength of the obtained nanocomposites was tested and the presence of nanofiller had a slight influence on the change in tensile strength (Fig. 2a). The presence of crystalline nanocellulose caused a minimal decrease in tensile strength, except for the addition of 2% by weight of nanocellulose, where a reduction of 10% was observed compared to the unfilled P3HB. Similarly, the reduction of the strain at break was observed (Fig. 2b). After adding the nanoadditive, the strain at break decreased by approx. 10% and the value fluctuated around 3 %, regardless of the amount of nanocellulose. In the case of testing the impact strength of the produced nanocomposites (Fig. 2c), it was noticeable that the impact strength decreased with increasing the nanocellulose content from 0.5 to 2% by weight. It would suggest a stiffening effect of the nanoadditive. However, the use of 3 wt.%. of nanocellulose caused a renewed increase in the impact strength almost to the impact value of the unfilled P3HB.A clear increase in the hardness of the produced nanocomposites (Fig. 2d) by an average of 10% was observed, indicating the stiffening of the structure of the produced materials.In order to examine the durability, and the processing and functional properties of the obtained nanomaterials, a thermogravimetric analysis, TGA, (Fig. 3) was carried out. TG curves of nanocomposites showed that thermal stability of all nanocomposites is higher than that of the unfilled P3HB. Introduction of nanocrystalline cellulose into P3HB matrix causes the increase of the degradation temperature of nanocomposites in reference to the unfilled P3HB e.g. 2% mass loss takes place at temperature 222.8°C. For the obtained nanocomposites the degradation temperature reported in the same conditions equaled 248.6, 248.1, 232.1, and 220.0°C in the case of P3HB-0.5, P3HB-1, P3HB-2 and P3HB-3, respectively. It can be observed that the weight loss temperature decreases with the increasing content of nanocrystalline cellulose in polymeric matrix. The addition of 0.5% or 1% mass of nanofiller increases the degradation temperature of nanocomposites by about 26°C in reference to the unfilled P3HB.The changes of the thermal properties of obtained composites were also studied using standard differential scanning calorimetry (DSC). Figure 4 shows the comparison of the experimental heat flow rate vs temperature of P3HB and the nanocomposites (0.5, 1, 2, 3 wt %) obtained based on the heating rate of 10°C/min in temperature range of -90°C to 195°C after prior cooling in the same rate from temperature range of 195°C to -90°C.The qualitative thermal analysis was carried out based on the heat flow rate of the semicrystalline P3HB and its nanocomposites. The glass transition and the melting were observed during the heating scan for all materials. The cold crystallization was recorded between the glass transition and melting region for P3HB-1, P3HB-2, and P3HB-3 (see Figure 4). All thermal parameters of phase transitions were estimated and listed in Table 2. The change of heat capacity at T_g, ΔC_p, and the temperature glass transition, T_g, were established based on the study of the glass transition region under heating and the heat of fusion, ΔH_f, and the melting temperature, T_{m1} and T_{m2}, were also estimated based on the analysis of melting region. Additionally, it can be seen that the double melting peak was maintained like for the P3HB analysis. It is probably related to the presence of crystals of different lamella thickness [18].

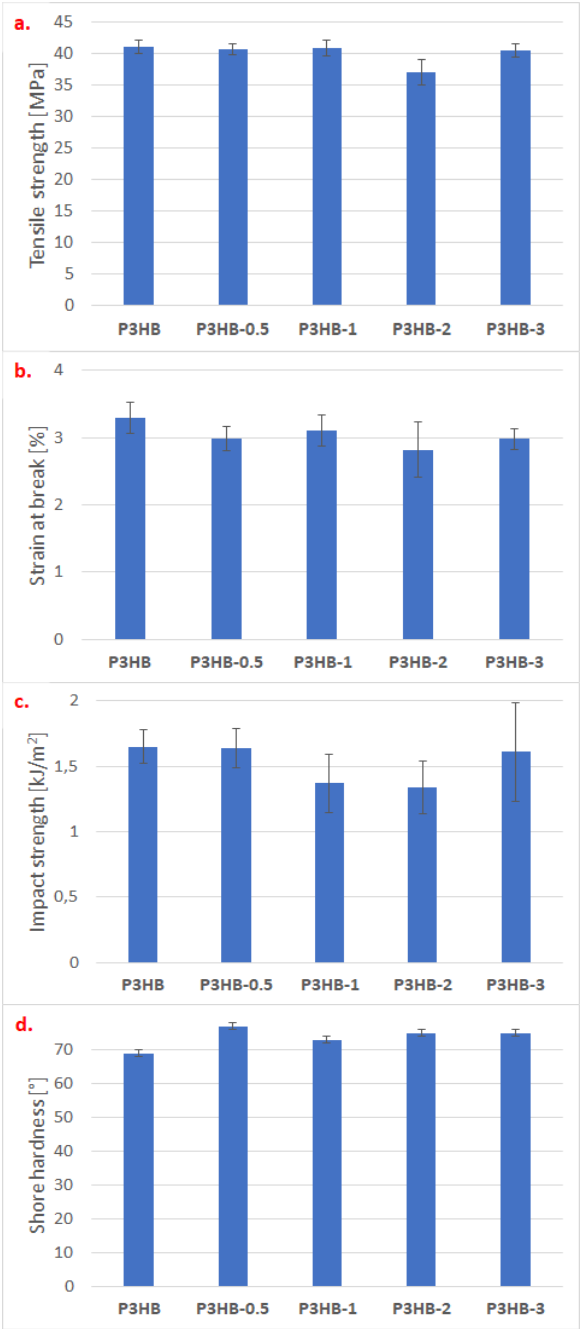


Fig. 2. Effect of nanocrystalline cellulose content on the tensile strength (a), strain at break (b), impact strength (c), and Shore hardness (d) of P3HB and its nanocomposites containing 0.5 and 1, 2, and 3 wt.% (designated P3HB-0.5, P3HB-1, P3HB-2, and P3HB-3, respectively).

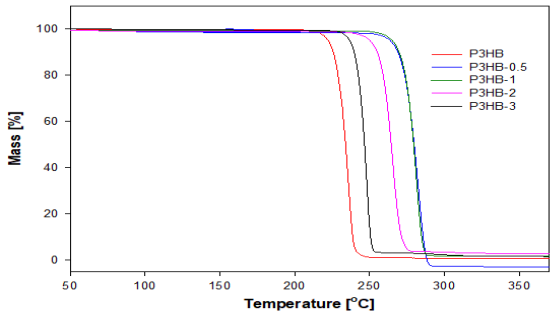


Fig. 3. TG analysis of the unfilled P3HB and their nanocomposites containing 0.5, 1, 2 and 3 mass/% of nanocrystalline cellulose (they were marked as P3HB-0.5, P3HB-1, P3HB-2, P3HB-3, respectively).

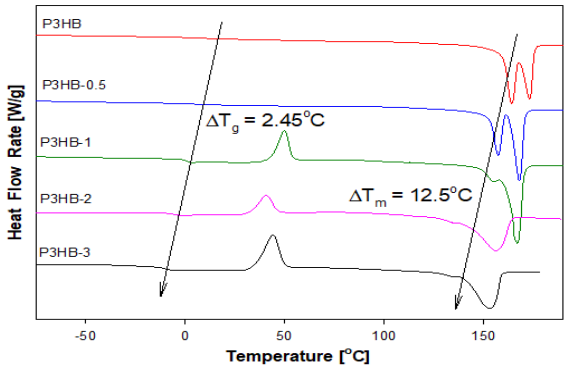


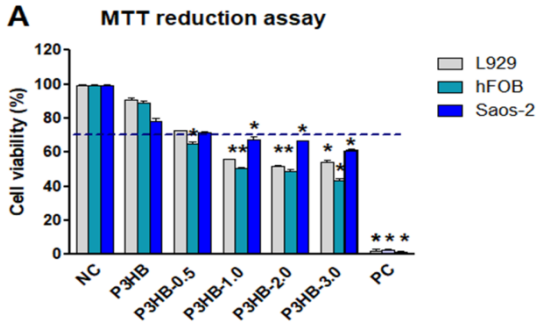
Fig. 4. Heat flow rate vs temperature obtained based on the DSC analysis of the unfilled P3HB and its nanocomposites containing 0.5, 1, 2 and 3 mass % of nanocrystalline cellulose (they were marked as P3HB-0.5, P3HB-1, P3HB-2, P3HB-3, respectively). The results were obtained during heating at 10 °C/min after cooling the sample at a constant rate of 10°C/min from melt

	T_g [°C]	C_p [J·g^{-1}·°C^{-1}]	T_{m1} [°C]	T_{m2} [°C]	H_f [J·g^{-1}]
P3HB	7.7	0,1768	-	165.80	100.36
P3HB-0.5	7.4	0.2565	157.30	167.90	87.68
P3HB-1	0.6	0.4926	155.45	166.60	8.02
P3HB-2	-5.7	0.2863	134.40	156.30	21.22
P3HB-3	-10.15	0.4932	134.20	153.30	1.945

Table 2. Comparison of the thermal parameters of the P3HB composites with nanocomposites of representative samples obtained while heating at a rate of 10°C·min^{-1} after cooling at the same rate.

The effect of the nanocrystalline cellulose additive on the glass transition temperature (T_g), and melting temperature (T_m), and the variations of heat of fusion and the heat capacity at T_g were investigated. Figure 4 shows the curves of the unfilled P3HB and its nanocomposites with a different content of nanofiller. It can be observed that the values of glass transition, and the melting temperature decreased with increasing contents of nanofillers.

The change of glass transition temperature and the change of melting temperature reached 2.45°C and 12.5°C, respectively. The variation of glass transition temperature for nanocomposite based on the highest amount of nanofiller in comparison with the unfilled P3HB equals 17.85°C. These relationships confirm the good dispersion of nanofiller in the polymeric matrix as reported earlier [19]. The decrease of the glass transition temperature of the composite, compared to unfilled P3HB, with increasing amounts of introduced nanofiller indicates the plasticizing effect of the nanocrystalline cellulose in reference to unfilled P3HB.In order to determine the application possibilities of the newly obtained nanocomposites, the cell viability and immunocompatibility in the milieu of tested materials were also carried out. The influence of P3HB, P3HB-0.5, P3HB-1, P3HB-2, P3HB-3 the viability of the reference L929 mouse fibroblasts and human hFBO 1.19 and Saos-2 was assessed by MTT reduction assay, based on the measurement of mitochondrial dehydrogenase activity in the presence or absence of the tested substances. In this assay, the biochemical activity of mitochondrial enzymes was positively correlated with cell viability.The viability of L929, hFOB 1.19 and Saoc-2 incubated with P3HB, and P3HB-0.5, (for all tested lines L929, hFOB 1.19 , Saos-2 cells) was higher than 70%, meeting the biological safety standard (Fig. 5A). For biomaterials (L929 and hFOb 1.19 cell line) P3HB-0.5, (hFOb 1.19 cell line) and P3HB-1.0, P3HB-2.0, P3HB-3.0 (for all tested cell line) do not meet the biosafety condition, cell viability below 70% (Fig. 5A). Monocytes are the most sensitive cells, and upon activation rapidly induce a cascade of inflammatory response. Only controlled inflammation leads to revascularization and regeneration of injured tissue. However, strong activation of monocytes by the components of the biomaterial or contaminants such as endotoxins may induce acute inflammation, potentially resulting in pus formation, tissue degradation, and disintegration of cell barriers [20]. THP1-Blue™ cells, like other monocytes, respond to ligands, such as peptides, endotoxins, and glycoconjugates, through toll-like receptors (TLR): TLR-2, TLR-4, TLR-5, TLR-6, and TLR-8. Upon TLR stimulation, NF-κB is activated, and the SEAP enzymatic marker is subsequently secreted into the cell culture milieu. In this study, we show that in the milieu of LPS THP-1xBlue monocytes responded by a high level of SEAP indicating the activation of nuclear transcription factor NF-kappa B.



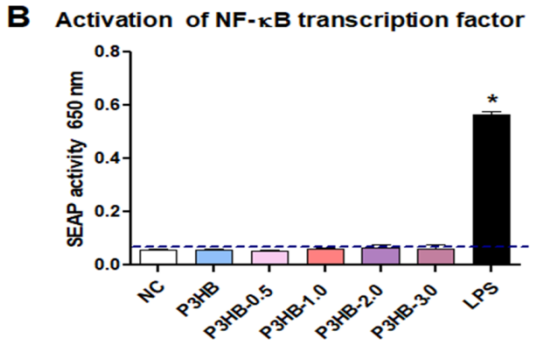


Fig. 5. Biocompatibility and immunocompatibility of P3HB, P3HB-0.5, P3HB-1, P3HB-2, P3HB-3.

A Cytotoxity the P3HB, P3HB-0.5, P3HB-1, P3HB-2, P3HB-3, towards mouse L929 and human hFob 1.19 and Saos-2 was estimated as percent of cells, which were able to reduce tetrazolium salt (3-(4,5-Dimethylthiazol-2-yl)-2,5-Diphenyltetrazoliu m Bromide) (MTT). NC – negative control (cells treated with H2O2), PC-positive control (cells in medium alone). Results are shown as mean ± standard deviation (SD). Three experiments were performed in triplicates for each experimental variant. The red line indicates the minimal percentage of viable cells (70%) required to confirm the extracts as non-cytotoxic at the in vitro level. Statistical analysis was performed using the nonparametric U Mann-Whitney test with significance, $p < 0.05$ (*unstimulated cells vs. stimulated cells).

B Activation of embryonic alkaline phosphatase (SEAP) in THP-1 x Blue monocytes. THP-1 x Blue monocytes were stimulated with lipopolysaccharide (LPS) E. coli alone, or P3HB, P3HB-0.5, P3HB-1, P3HB-2, P3HB-3. Control cells were subcultured in the medium alone. The supernatants were collected for assessment SEAP calorimetrically. The experiments were performed three times in triplicate for each experimental variant. The results are shown as mean ± standard deviation (SD). Statistical analysis was performed using the nonparametric U Mann-Whitney test with significance, $p < 0.05$ (*unstimulated cells vs. stimulated cells).

The P3HB, P3HB-0.5, P3HB-1, P3HB-2, P3HB-3 did not induced SEAP activity in none of the test concentrations beyond the negative control value of cells grown in medium alone, which confirmed the immunosafety of the tested extracts and the absence of, or very low, endotoxin contamination, which, according to the Food and Drug Agency Guidance as well as the European Medicines Agency, cannot be higher than 0.25 EU in biomaterials in contact with human blood/tissue. Based on our optimization study, the activation of THP1-Blue™ monocytes with 0.25 EU of endotoxin (positive control of monocyte activation) resulted in a significant increase in SEAP production, as shown by an absorbance of 1.5 ± 0.02 at 620 nm (Fig. 5B).

VI. CONCLUSION

The nanocomposites of P3HB and nanocrystalline cellulose were obtained during direct mixing in a co-rotating twin-screw micro-extruder. The conducted studies revealed clearly the influence of nanofiller in the P3HB matrix on the selected thermal, mechanical and biological properties of the prepared nanocomposites. It has been observed that the introduction of nanocrystalline cellulose into a polymeric matrix influences the better thermal stability of the nanocomposites, measured by TG, under non-oxidative conditions. The best thermal stability was observed for the P3HB-0.5 and P3HB-1 and was comparable to the degradation temperature value of 2% weight loss. The presented thermal analysis showed a decrease in the glass transition and melting temperatures with an increasing amount of nanofillers in the obtained P3HB composites. The decrease in the melting temperature of the nanocomposites is preferred due to the fact that so-called the processing window is widened, which gives better processing possibilities of the obtained nanocomposites in relation to unfilled P3HB. It can be seen that the best thermal properties and the widest processing window expressed as the difference between the degradation temperature and the melting temperature were obtained for P3HB-1 and relatively similarly for P3HB-0.5 and were 81.5 and 80.7°C, respectively. This movement apart from melting and decomposition temperatures of nanocomposites based on P3HB facilitates processing and prevents the degradation of the material.Additionally, introducing nanocrystalline cellulose into a P3HB matrix leads to an increased degree of crystallinity of the nanocomposites. The X-ray spectra confirmed the crystallinity growth of the obtained nanocomposites. This phenomenon is due to the increase in crystal number as the nanocrystalline cellulose percentage is higher.Mechanical and thermal tests showed that the most desirable properties oscillate around P3HB-0.5 and P3HB-1, indicating the advantage of P3HB-1, which displays the most plastic character in relation to P3HB. However, biological studies in terms of implant applications have shown that only P3HB-0.5 can be of key importance. Theimmunosafety of the tested extracts and the absence of, or very low, endotoxin contamination was confirmed by the Food and Drug Agency Guidance as well as the European Medicines Agency.

REFERENCES

[1] J. Delayey, P. Dubruel, V. Vlierberghe, „Shape-Memory Polymers for Biomedical Applications," Advanced Functional Materials vol. 30, 44.

[2] M. Behl, and A. Lendlein, „Shape-memory polymers," Mater today, vol. 10, pp. 20-28, 2000.

[3] C. Wischke, A. Neffe, S.Steuer, and A. Lendlei, „Evaluation of a degradable shape-polymer network as matrix for controlled drug release," J Control Release, vol. 138, pp. 243-250, 2009.

[4] D. Ratna, and J. Karger-Kocsis, „Recent advances in shape memory polymers and composites: a review," J Mater Sci, vol. 43, pp. 264-265, 2008.
[5] K. Dyamenahalli, A. Famili, and R. Shandas, „3 - Characterization of shape-memory polymers for biomedical applications," Shape Memory Polymers for Biomedical Applications Woodhead Publishing Series in Biomaterials, pp. 35-63, 2015.
[6] X. Zhai, Y. Ma, C. Hou, F. Gao, Y. Zhang, C. Ruan, H. Pan, W. W. Lu, and W. Liu, „3D-Printed High Strength Bioactive Supramolecular Polymer/Clay Nanocomposite Hydrogel Scaffold for Bone Regeneration," ACS Biomater. Sci. Eng., vol. 3, 6, pp. 1109-1118, 2017.
[7] H. Xuan, H. Hu, C. Geng, J. Song, Y. Shen, D. Lei, Q. Guan, S. Zhao, and Z. You, „Biofunctionalized chondrogenic shapememory ternary scaffolds for efficient cell-free cartilage regeneration," Acta Biomater., vol. 105, pp. 97-110, 2020.
[8] R. Kłosek, J. Komacki, A. Orchel, and Z. Dzierżewicz, „ShapeMemoryPolymers In Biomedical Applications," Farm Przegl Nauk, vol. 11, pp. 39-44, 2010.
[9] G. Chen, and Q. Wu, „The application of polyhydroxyalkanoates as tissue engineering materials," Biomaterials, vol. 26, pp. 6565–6571, 2005.
[10] E. Szewczuk., „Biodegradowalne poliestry hydroksykwasów alkanowych (PHA) syntetyzowane przez drobnoustroje," Biotechnologia, vol. 3, 34, pp. 98-115, 1996.
[11] V. Sastri, „Chapter 9 - Other Polymers: Styrenics, Silicones, Thermoplastic Elastomers, Biopolymers, and Thermosets, Plastics in Medical Devices. Properties, Requirements, And Applications," Plastics Design Library, pp. 217-262, 2010.
[12] G. Polotti, „Chapter Eight - Perspectives from industry," Advances in Chemical Engineering, vol. 56, 1, pp. 259-330, 2020.
[13] S. Baidurah, and T. Kobayashi, „ Polyhydroxyalkanoates: Production and Biodegradation - A Review," Encyclopedia of Materials: Plastics and Polymers, vol. 2, pp. 530-540, 2022.
[14] F. Hempel, A. Bozarth, N. Lindenkamp, A. Klingl, S. Zauner, U. Linne, A. Steinbüchel, and U.G. Maier, „Microalgae as bioreactors for bioplastic production," Microb. Cell Factories, vol. 10, pp. 81–86, 2011.
[15] A. Czerniecka-Kubicka, I. Zarzyka, and M. Pyda, „Advanced analysis of poly(3-hydroxybutyrate) phases based on vibrational heat capacity," J Therm Anal Calorim, vol. 127, pp. 905–914, 2017.
[16] Brzeziński, M.; Kost, B.; Gonciarz, W.; Krupa, A.; Socka, M.; Rogala, M. Nanocarriers based on block copolymers of l-proline and lactide: The effect of core crosslinking versus its pH-sensitivity on their cellular uptake. Eur. Polym. J. 2021, 156, 110572.
[17] Gonciarz, W.; Matusiak, A.; Rudnicka, K.; Rechciński, T.; Chałubiński, M.; Czkwianianc, E.; Brolnel, M.; Chmiela, M. Autoantibodiesto a specific peptide epitope of human Hsp60 (ATVLA) with homology to Helicobacter pylori HspB in H. pylori-infectedpatients. APMIS 2019, 127, 139–149.
[18] A. Czerniecka-Kubicka, I. Zarzyka, M. Pyda. Journal of Thermal Analysis and Calorimetry 127 (2017) 905 – 914
[19] Hablot E, Bordes P, Pollet E, Averous L. Thermal and thermomechanical degradation of poly(3-hydroxybutyrate)-based multiphase systems. Polym Degrad Stab. 2008;93:413–21.
[20] Mantovani A.; Biswas S.K.; Galdiero M.R.; Sica A.; Locati M. Macrophage plasticity and polarization in tissue repair and remodelling. The Journal of Pathology, 2013, 229, 176–185. doi:10.1002/path.4133

★★★